

HYDROLYSIS OF MANGANESE CARBIDES Mn_5C_2 AND $Mn_{23}C_6$ *

Pavel KAREN and Bohumil HÁJEK

*Department of Inorganic Chemistry,**Prague Institute of Chemical Technology, 166 28 Prague 6*

Received September 17th, 1985

Diffractionally pure manganese carbides Mn_5C_2 and $Mn_{23}C_6$ were hydrolyzed with water at 25 and 60°C. Based on the model of contracting spherical particles in the carbide powder particulate system, the corrosion rates were calculated from the course of gas evolution during the hydrolysis; the values obtained were as follows in $\mu\text{m/h}$: Mn_5C_2 : 1.2 ± 0.4 at 25°C and 10 ± 3 at 60°C, and $Mn_{23}C_6$: 0.15 ± 0.01 at 25°C and 2.2 ± 0.2 at 60°C. The hydrolysis gives rise to hydrogen and a concentration-decreasing sequence of predominantly saturated hydrocarbons, the fraction of C_2 and higher hydrocarbons being about 6 times lower for $Mn_{23}C_6$ than for Mn_5C_2 . The hydrogen and hydrocarbon contents of the mixture after hydrolysis are consistent with the assumed reaction course, where the adsorbed active hydrogen, formed during the hydrolysis reaction due to the "metallic" nature of the carbide, partly reacts with the methane arising from the hydrolysis of the C_1 groups in the carbide and partly combines to molecular hydrogen.

Manganese carbides differ from carbides of the neighbouring transition metals of the *d*-series in their hydrolyzability by water or air humidity¹. The carbon atoms in the structures of manganese carbides²⁻⁶ Mn_7C_3 , Mn_5C_2 , Mn_3C , $Mn_{15}C_4$, and $Mn_{23}C_6$ are located in the prisms of the manganese atoms so that C—C bonding interactions are ruled out. In spite of this, their hydrolysis does not give rise to a single hydrocarbon, methane, accompanied by hydrogen according to the carbide stoichiometry^{7,8}. In the literature data on the hydrolysis of manganese carbides, the composition of the hydrolysis products never corresponded to the stoichiometry of the hydrolyzable carbide concerned (except for Mn_3C , ref.⁷). Therefore, in^{9,10} we studied the hydrolysis of Mn_7C_3 , which was found to result in the formation of hydrogen, saturated hydrocarbons in a concentration-decreasing sequence, and a similar sequence of olefins in trace concentrations. Based on a comparison of the results of hydrolysis of uranium monocarbide samples of different compositions, UC_{1-x} , we devised¹¹ a model for the hydrolysis reaction of these carbides, where the key role is ascribed to the hydrogen formed by the reaction of the carbide with water: the nascent hydrogen partly combines to H_2 and partly reacts with the methane formed by the hydrolysis, giving hydrocarbon radicals and additional

* Part XXIX in the series Studies on Hydrolyzable Carbides; Part XXVIII: This Journal 51, 1411 (1986).

molecular hydrogen. The amount of the latter in the gas mixture is thereby increased above the value corresponding to the formation of hydrogen besides methane. The more extensive is the transfer reaction of H with lower hydrocarbons, the higher will be the amount of hydrogen and higher hydrocarbons, formed by recombination of the radicals, in the final gas product. To prove whether the extent of the reaction of H with CH_4 will be different for carbides with different compositions, determining the H-to- CH_4 ratio in the primary mixture, we chose two manganese carbides such that for the one, Mn_5C_2 , the amount of H and CH_4 in the primary mixture is the same, whereas for the other, Mn_{23}C_6 , the amount of H exceeds substantially that of CH_4 .

EXPERIMENTAL

Carbide synthesis. Manganese metal (coarse powder) 99.9% (Lachema, Brno) and granulated carbon black 99.99% (Pramet, Šumperk) were homogenized by grinding under n-heptane for 72 h in a tungsten carbide mill. The powder emerging (micrometer particle size) was compressed into pellets, which were heated for 600 h at 900°C in a tantalum container accommodated in a sealed quartz ampoule. The 1 kPa argon atmosphere in the ampoule was gettered by means of chips of a misch metal, placed in a corundum crucible in the hot zone above the tantalum container.

Chemical and X-ray diffraction analysis of samples. The analyses were performed as described previously⁹.

Hydrolysis. About 0.1 g of carbide powder sample was decomposed with water in evacuated 10 ml ampoules at 25 and 60°C . The composition of the gaseous product was determined gas chromatographically on a Hewlett-Packard 5840A instrument equipped with a thermal conductivity detector, using helium as carrier gas. The calibration was performed by means of a mixture of a natural gas standard (Linde) and hydrogen. Details have been reported⁹. The hydrolysis rate was measured from the volume of the gas formed. The carbides were decomposed similarly as given above, the starting atmospheric pressure in the ampoule was adjusted with argon. The sample was not stirred during the decomposition. The particle size of the starting carbide powder was monitored, for determining the corrosion losses, with an MV-2 image analyzer (Opton, Oberkochen).

RESULTS AND DISCUSSION

Preparation and Composition of Carbides

X-ray diffractographically pure Mn_5C_2 ($C2/c$, $a = (1\,167 \pm 0.2)$ pm, $b = (458.35 \pm 0.12)$ pm, $c = (509.5 \pm 0.1)$ pm, $\beta = (97.71 \pm 0.01)^\circ$, $Z = 4$) and Mn_{23}C_6 ($Fm\bar{3}m$, $a = 1\,059.46 \pm 0.04$ pm, $Z = 4$) were prepared. The two samples were apparently crystalline, with metallic lustre. Mn_{23}C_6 was compact and brittle, Mn_5C_2 pellets were macroscopically porous. The results of chemical analysis (Table I) are consistent with the formulae. The presence of oxygen is due to contamination of the starting metal powder and by partial hydrolysis of the carbide by air humidity during the sample handling for its analysis.

Hydrolyzability of Mn_5C_2 and $Mn_{23}C_6$

The corrosion rate of the particulate carbide system was calculated from the extent of reaction of the carbide with water (ξ), which corresponds to the fraction of gas formed in time t with respect to the total amount of gas evolved, owing to the fact that virtually only saturated hydrocarbons arise. The carbide particles were roughly spherical in shape; two-dimensional analysis gave length-to-breadth ratios of approximately 0.9 for the two samples. The results of particle size analysis for $Mn_{23}C_6$ powder are shown in Fig. 1, the data for Mn_5C_2 are similar.

With regard to the relatively slow course of hydrolysis, the chemical reaction was assumed to be the controlling step. So, the model of contracting spherical particles could be applied (Fig. 2). Here the rate of change in the particle radius, dr_a/dt (where r_a is the instantaneous particle radius and t is reaction time) is assumed to be constant¹²,

$$-dr_a/dt = \text{const.} \quad (1)$$

The extent of reaction ξ for a contracting sphere depends on the initial and instantaneous particle radii R and r_a , respectively, as

$$\xi = 1 - (r_a/R)^3. \quad (2)$$

In the system of particles of different size, the contributions to the ξ value from the separate particle groups (columns in the histogram in Fig. 1) have to be considered, so that

$$\xi = 1 - \sum_{i=1}^n x_i(A_i)^3, \quad (3)$$

TABLE I

Results of chemical analysis of the carbides prepared

Element	Mn_5C_2		$Mn_{23}C_6$	
	Calculated %	Found %	Calculated %	Found %
Mn	91.96	92.0 ± 0.2	94.6	94.6 ± 0.2
C	8.04	7.75 ± 0.1	5.4	5.2 ± 0.1
O	—	0.3 ± 0.05	—	0.4 ± 0.05
Total	100.00	100.5	100.0	100.2

where x_i is the weight (volume) fraction of particles of the i -th column with the mean initial radius \bar{R}_i , n is the total number of columns in the histogram, and A_i is $1 - (l_c/\bar{R}_i)t$ if $t < (\bar{R}_i/l_c)$ and zero if $t \geq (\bar{R}_i/l_c)$; l_c is the linear corrosion loss per time unit ($l_c = -dr_a/dt$). The one of the l_c roots that has physical sense is calculated from this equation.

It follows from the results given in Table II that the corrosion rate is higher for the carbide with the higher carbon content. The corrosion rate of Mn_5C_2 calculated

TABLE II

Linear corrosion loss of manganese carbides during their reaction with liquid water at 25°C and 60°C in unstirred medium

Extent of reaction ξ	Corrosion loss, $\mu\text{m h}^{-1}$			
	Mn_5C_2		$Mn_{23}C_6$	
	25°C	60°C	25°C	60°C
0.2	0.83	7.0	0.15	2.4
0.5	1.2	10.0	0.14	2.10
0.8	1.6	12.2	0.16	2.05

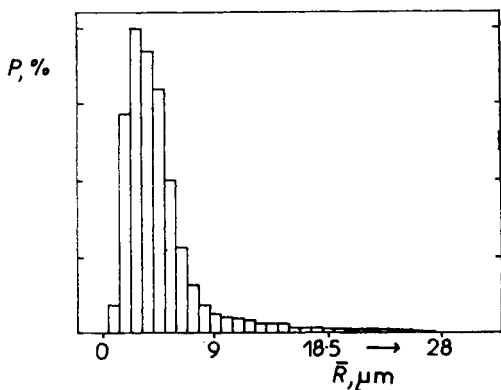


FIG. 1

Size analysis of the $Mn_{23}C_6$ particulate system; histogram of number of particles (P) by the mean particle radius (\bar{R}), step 0.95 μm

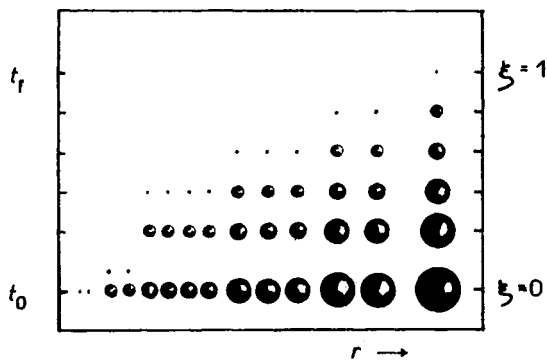


FIG. 2

Model of spherical particles of the carbides contracting during the hydrolysis in dependence on time (t_f is the final time)

within the scope of this model increases slightly as the reaction proceeds, presumably due to corrosion at the grain boundary and to decomposition of the particles, as is consistent with the morphology of the Mn_5C_2 powder. For the very compact $Mn_{23}C_6$, the corrosion rate at 25°C was roughly constant over the whole reaction period, whereas at 60°C, a slowdown of the reaction was observed, which may be associated with the diffusion of water through the amorphous voluminous $Mn(OH)_2 \cdot xH_2O$.

Composition of Hydrolysis Products

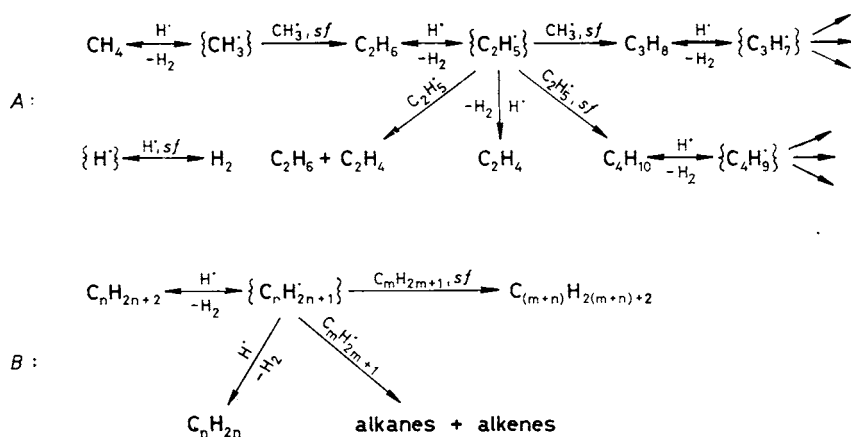
Similarly as for Mn_7C_3 (refs^{9,10}) and UC_{1-x} (ref.¹¹), the composition of the gas mixture after the hydrolysis of Mn_5C_2 and $Mn_{23}C_6$ (Table III) is characterized by the occurrence of a homologous series of saturated hydrocarbons whose concentrations decrease with increasing number of carbon atoms in their molecules. The fraction of methane homologues is higher for Mn_5C_2 than for $Mn_{23}C_6$ and, for both carbides, at lower temperatures of hydrolysis than at higher temperatures.

The decreasing trend of concentrations of hydrocarbons in the series is consistent with the decreasing probability of their formation, as follows from Scheme 1 for

TABLE III
Composition of gaseous products of hydrolysis of Mn_5C_2 and $Mn_{23}C_6$ (%(V/V))

Component	Mn_5C_2		$Mn_{23}C_6$	
	20°C	60°C	20°C	60°C
H_2	53.8	51.0	70.3	67.5
CH_4	28.7	34.1	25.5	30.1
C_2H_6	15.3	13.1	3.64	2.07
C_2H_4	0.128	0.080	0.043	0.017
C_3H_8	1.63	1.40	0.683	0.261
C_3H_6	0.016	—	0.013	0.014
<i>i</i> - C_4H_{10}	0.052	0.037	0.011	0.004
<i>n</i> - C_4H_{10}	0.267	0.130	0.055	0.020
C_4H_8	0.050	0.018	0.006	0.001
<i>i</i> - C_5H_{12}	0.022	0.005	0.005	0.0006
<i>n</i> - C_5H_{12}	0.040	0.004	0.006	0.001
C_6	0.021	0.023	0.008	0.007
H/C	5.00	5.04	7.666	7.673
s^a	0.613	0.53	0.086	0.043

^a Eq. (4).



SCHEME 1

the assumed radical reactions proceeding from methane, formed by the hydrolysis of carbide of methanide type, and nascent hydrogen (*A* initial stage; *B* generally; intermediates of hydrolysis are given in brackets; *sf* means that a third molecule or a solid surface need to participate). Since, within the scope of the concept proposed, it is the nascent hydrogen that is responsible for the course of the radical reactions, it is convenient to look upon the composition of the final gas mixture as if a fraction *s* ($s \in (0, 1)$) out of 1 mole of the initially formed H had reacted with hydrocarbons (methane in particular) according to Scheme 1, while the remaining fraction $(1 - s)$ had recombined to H_2 (see the total balance in Fig. 3).

Expressing the mole fraction of hydrogen x_{H_2} from the diagram in Fig. 3 and the amount of methane and H in the primary mixture in terms of the H/C ratio, we obtain

$$x_{\text{H}_2} = (1 + s)(\text{H/C} - 4)/(\text{H/C} - 2); \quad (4)$$

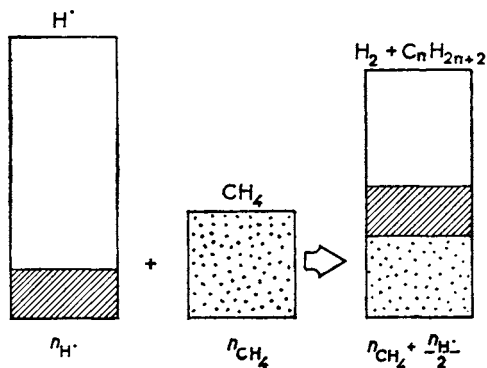


FIG. 3

Total substance balance of carbide hydrolysis reactions for the starting components H and CH_4 . Hatched: $s \cdot n_{\text{H}}$ moles of hydrogen H that reacted with hydrocarbons, and the corresponding amount of H_2 in the final mixture; dotted: CH_4 and hydrocarbons

for $H/C > 5$, $s \leq 1/(H/C - 4)$ because the amount of H to react with methane cannot exceed the amount of the latter.

The values of s calculated from the compositions of the gas mixtures (Table III) are roughly proportional to the concentrations of methane in the primary mixtures with hydrogen (if s were equal to x_{CH_4} in the initial mixture, x_{H_2} would be equal to $(H/C - 4)/(H/C - 3)$). It follows from the overall balance of the reactions of hydrogen and hydrocarbons in Fig. 4 for $Mn_{23}C_6$ and Mn_5C_2 , and also from our study of Mn_7C_3 , that s decreases with decreasing methane content, a considerable drop being observed if the amount of H in the primary mixture exceeds that of methane, *i.e.*, if $H/C > 5$. The high concentration of H then probably causes termination of a large fraction of CH_3 radicals by trimolecular collisions with H. This termination is favoured by increased temperature, as is indicated by the lower fraction of C_2 and higher hydrocarbons in the gas after hydrolysis of the carbide at $60^\circ C$.

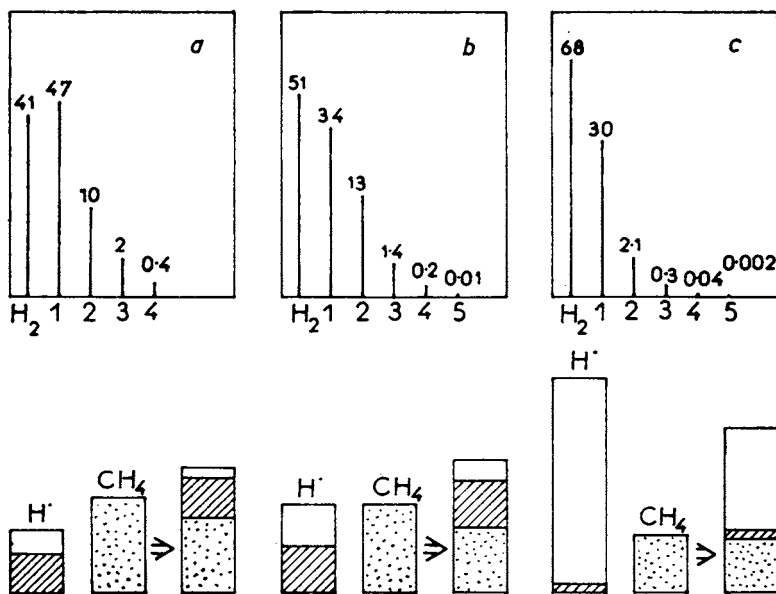


FIG. 4

Diagrams of composition of the gaseous products of hydrolysis of manganese carbides and the corresponding total substance balance, of reactions of radicals for the initial components H and CH_4 , per mol Mn. *a* Mn_7C_3 (ref.⁹), $(H/C)_{exp} = 4.67$; *b* Mn_5C_2 , $(H/C)_{exp} = 5.04$; *c* $Mn_{23}C_6$, $(H/C)_{exp} = 7.67$. Fractions of H_2 and saturated hydrocarbons of homologous series (labelled 1, 2, ...) in $(\%V/V)^{1/2}$. Hatched: fraction s of H^\cdot radicals and the corresponding amount of H_2 formed ($s = 0.62, 0.53, 0.043$, respectively); dotted: hydrocarbons

In principle, this concept can be basically extended also to other transition metal carbides whose hydrolysis gives rise to hydrocarbons and active hydrogen; however, it should be taken into account that effects other than the stoichiometry alone also participate in the control of the extent of the radical reactions. Among them it is the nature of the metal involved and the related higher or lower tendency of the carbide surface to adsorb or chemisorb radical species, which play a part in the formation of the hydrocarbon mixture. The fact that the radical reactions occurring during the hydrolysis are associated with the reaction surface was pointed out, for uranium monocarbide, by Bradley and Ferris as long as twenty years ago¹³.

REFERENCES

1. Hilpert S., Paunescu J.: *Ber. Deut. Chem. Ges.* **46**, 3479 (1913).
2. Rouault M., Herpin P., Fruchart M.: *Ann. Chim. (Paris)* **5**, 461 (1970).
3. Bouchaud J.-P.: *Ann. Chim. (Paris)* **2**, 353 (1967).
4. Kuo K., Person L. E.: *J. Iron Steel Inst.* **178**, 39 (1954).
5. Bowman A. K., Arnold G. P., Storms E. K., Nereson N. G.: *Acta Cryst.*, **B 28**, 3102 (1972).
6. Novik N. I., Taran J. N.: *Izv. Akad. Nauk SSSR, Neorg. Mater.* **13**, 1013 (1977).
7. Myers W. R., Fishel W. P.: *J. Amer. Chem. Soc.* **67**, 1962 (1945).
8. Domashevich L. T., Fenotschka B. V., Gordienko S. P., Timofeeva I. I., Karalnik S. M., Koval A. V., Kosolapova T. Ya. in the book: *Karbidy i Splavy na Ikh Osnove* (G. V. Samsonov, Ed.), p. 44. Naukova Dumka, Kiev 1976.
9. Hájek B., Karen P., Brožek V.: *This Journal* **48**, 2740 (1983).
10. Brožek V., Hájek B., Karen P., Matucha M., Žilka L.: *J. Radioanal. Chem.* **80**, 165 (1983).
11. Hájek B., Karen P., Brožek V.: *This Journal* **49**, 793 (1984).
12. Barret P.: *Cinétique Hétérogène* (Czech translation), p. 156. Academia, Prague 1978.
13. Bradley M. J., Ferris L. M.: *J. Inorg. Nucl. Chem.* **27**, 1557 (1965).

Translated by P. Adámek.